ANALOG CONTROLLER DESIGN FOR AN ACTIVE DAMPING ELEMENT

Jan Holterman, Job van Amerongen

Control Laboratory, Drebbel Institute for Mechatronics, University of Twente
PO Box 217, 7500 AE Enschede, The Netherlands
j.holterman@utwente.nl, j.vanamerongen@utwente.nl
http://www.ce.utwente.nl

Abstract: The 'Smart Disc' is an active structural element to be used for damping vibrations in high-precision machines. It is based on a piezoelectric position actuator and a collocated piezoelectric force sensor. Active damping is realised by a feedback loop. In order to miniaturise the electronics involved in the Smart Disc concept, the sensor amplifier, the controller electronics, and the actuator amplifier may be integrated into an analog circuit based on a single operational amplifier. Controller design then boils down to proper dimensioning of a first-order lowpass filter with three electric components: one capacitor and two resistors.

Keywords: vibration dampers, active control, robust control, decentralised control, analog control, electronics, charge amplifiers, lowpass filters.

1. INTRODUCTION

The Smart Disc project is aimed at the development of active structural elements to be used for damping vibrations in high-precision machines. This concept was successfully proven in the lens support of an advanced microlithography machine (Holterman, 2002). Design of a so-called 'Smart Disc' involves design of mechanics, electronics, and a controller.

Smart Disc mechanics. The Smart Disc concept is based on a position actuator in series with a force sensor. For the Smart Discs developed at the University of Twente, both the actuator and the sensor have been realised by means of piezoelectric material:
- the *force sensor* relies on the *direct* piezoelectric effect: upon application of a force, the piezoelectric material deforms and generates an electrical charge;
- the *position actuator* relies on the *indirect* piezoelectric effect: upon application of an electric field, the piezoelectric material deforms.

Smart Disc electronics. The electronics may be split up into three separate functional building blocks:
- a *sensor amplifier*, converting the charge from the sensor into an input voltage for the electronic controller, eventually equipped with an anti-aliasing filter if the controller is implemented digitally;
- an *electronic controller* (analog or digital);
- an *actuator amplifier*, converting the output voltage from the controller to a voltage (with sufficient power) that can be applied to the piezoelectric actuator.

Smart Disc control. During the project several control strategies were investigated. For reasons of flexibility these controllers were implemented digitally. The most straightforward method to implement active damping is to apply *Integral Force Feedback* (IFF), i.e., to implement an integrator in the feedback loop between sensor and actuator. To prevent actuator saturation for low frequencies, in

practice a leaking integrator is implemented rather than a pure integrator. It is in fact a first-order lowpass filter, with a cut-off frequency well below the first resonance frequency to be damped.

In order to end up with a stand-alone active structural element, the three electronic building blocks (sensor amplifier, control electronics, actuator amplifier) should ideally be combined into an as simple as possible electric circuit. When implemented in analog electronics, the before-mentioned anti-aliasing filter is superfluous. If for a particular application the power requirements of the actuator are low, the actuator amplifier may also be superfluous.

In the present paper it will be shown how the IFF-controller function can be incorporated in the charge amplifier of the sensor. In section 2 the basic idea behind active damping is discussed. It will be shown how the IFF-controller parameters should be tuned for proper damping of a single dominant vibration mode (section 3). The basic idea behind a charge amplifier is discussed Section 4. A procedure is presented for realisation of optimal IFF-control by properly dimensioning the electric components involved in the modified amplifier circuit. Practical use of this procedure is demonstrated for an experimental set-up (section 5).

2. ACTIVE DAMPING WITHIN THE SMART DISC CONCEPT

In order to illustrate the basic idea of active damping with a Smart Disc, we consider a piezoelectric actuator in series with a piezoelectric sensor, embedded in a certain mechanical structure (schematically depicted in the left part of Fig. 1). The actuator and the sensor can be modelled as an ideal position actuator and an ideal force sensor, in series with a single stiffness element that represents the limited stiffness of the piezoelectric material. The elastic force in the structure is measured (F_{sens}) and fed to the controller $C(s)$, which generates a desired position for the actuator (x_{act}), so as to damp the measured vibrations.

Note 1: The position actuator in Fig. 1 represents the *desired* elongation, i.e., the elongation of an *unloaded* actuator. The *true* elongation of the position actuator also depends on the mechanical conditions, i.e., on the actuator stiffness k_{act} and the externally applied force F_{ext}:

$$x_{\text{act}}^{\text{true}} = k_{\text{act}}^{-1} F_{\text{ext}} + x_{\text{act}}^{\text{unl}} \tag{1}$$

Note 2: In Fig. 1 the feedback idea is made explicit by introducing a zero force reference signal, such that $F_{\text{err}} = F_{\text{ref}} - F_{\text{sens}}$.

To achieve robust active damping, the only model knowledge needed, is that position actuator and force sensor are collocated. Here 'collocation' implies that the associated signals for the actuator and sensor are *power-conjugated*: the product of the actuated *velocity* and the measured *force* represents the *power* that is injected into the mechanical structure. This implies that, if we impose a static relation between measured force F_{sens} and actuated velocity v_{act}, we are effectively implementing a viscous damper. This behaviour is achieved by incorporating an integrator in the feedback loop, like illustrated in Fig. 1:

$$\begin{aligned} C(s) &= \frac{x_{\text{act}}(s)}{F_{\text{err}}(s)} = \frac{K_{\text{IFF}}}{s} \\ \rightarrow \quad x_{\text{act}}(s) &= \frac{K_{\text{IFF}}}{s} F_{\text{err}}(s) \\ \rightarrow \quad v_{\text{act}}(s) &= K_{\text{IFF}} F_{\text{err}}(s) \end{aligned} \tag{2}$$

This active damping strategy is referred to as *Integral Force Feedback* (IFF; Preumont *et al.*, 1992).

For a look from the perspective of controller design, consider the open-loop Smart Disc transfer function:

$$H_{\text{SD}}(s) = \frac{F_{\text{sens}}}{x_{\text{act}}}(s) \tag{3}$$

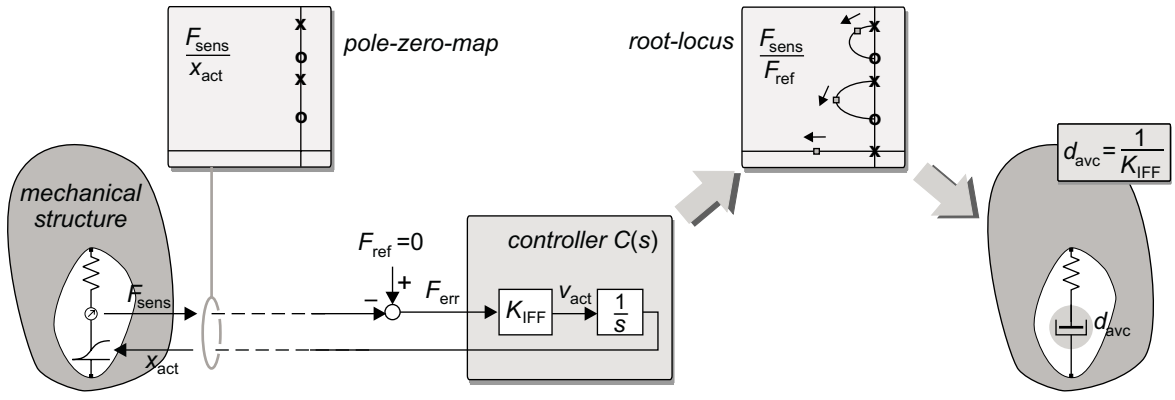

Fig. 1. The Smart Disc frequency response, from position actuator to collocated force sensor, is characterised by an alternating pole-zero-pattern. Upon application of Integral Force Feedback, all resonances are damped (poles moving into the left half of the s-plane). The Smart Disc then effectively behaves as a viscous damper.

In the absence of structural damping, the pole-zero-map of this transfer function is characterised by poles and zeros on the imaginary axis. For a collocated actuator-sensor-pair, it can be shown that the pole-zero-map exhibits an *alternating* pole-zero-pattern (Preumont, 1997). This is illustrated in the upper-left part of Fig. 1 for a mechanical structure with two vibration modes (i.e., two pairs of poles and zeros). By adding an extra pole in the origin (the integrator in the feedback loop), all branches of the root-locus are drawn into the left half of the s-plane. This implies that all resonances are damped (robustly, as hardly any model knowledge has been used). See the upper-right part of Fig. 1.

A first-order lowpass filter, with cut-off frequency well below the first resonance frequency to be damped, is implemented rather than a pure integrator:

$$C(s) = \frac{K_{\mathrm{IFF}}}{s + p_{\mathrm{IFF}}} \tag{4}$$

This control law (so-called *leaking IFF*; Holterman, 2002) implements the behaviour of a stiffness element,

$$k_{\mathrm{avc}} = \frac{p_{\mathrm{IFF}}}{K_{\mathrm{IFF}}} \tag{5}$$

in parallel with the damper d_{avc}. Optimal controller design thus effectively boils down to a *stiffness-versus-damping trade-off*: balancing between appropriate behaviour for low frequencies ('stiffness') and appropriate damping for higher frequencies, where the resonances occur.

3. CONTROLLER DESIGN FOR SINGLE-MODE DAMPING

We consider the design of an IFF-controller for a mechanical structure characterised by a single dominant vibration mode. In that case, the transfer function from actuated position x_{act} to measured force F_{sens} is given by (the general shape is shown in the upper plot in Fig. 2):

$$H_{\mathrm{SD}}(s) = \frac{F_{\mathrm{sens}}}{x_{\mathrm{act}}}(s) = k_{\mathrm{int}}^{\mathrm{bl}} \frac{s^2 + \omega_{\mathrm{a}}^2}{s^2 + \omega_{\mathrm{e}}^2} \tag{6}$$

with:
- ω_{e} : the dominant resonance frequency;
- ω_{a} : the dominant anti-resonance frequency;
- $k_{\mathrm{int}}^{\mathrm{bl}}$: the internal stiffness that is experienced for high frequencies ($\omega \gg \omega_{\mathrm{e}}$; 'blocked' situation).

Under the assumption that the piezoelectric stack does not suffer from direct electric feed through from actuator to sensor, the transfer function from actuator voltage U_{act} to sensor charge q_{sens}, is given by (see upper plot in Fig. 2):

$$H_{\mathrm{SD}}^{\mathrm{el}}(s) = \frac{q_{\mathrm{sens}}}{U_{\mathrm{act}}}(s) = K_{\mathrm{SD}}^{\mathrm{hf}} \frac{s^2 + \omega_{\mathrm{a}}^2}{s^2 + \omega_{\mathrm{e}}^2} \tag{7}$$

with the gain for high frequencies given by:

$$K_{\mathrm{SD}}^{\mathrm{hf}} = d_{\mathrm{s}} k_{\mathrm{int}}^{\mathrm{bl}} d_{\mathrm{a}} \tag{8}$$

with:
- d_{s}: the piezoelectric charge constant of the sensor (electric charge = $d_{\mathrm{s}} \times$ force);
- d_{a}: the piezoelectric charge constant of the actuator (mechanical displacement = $d_{\mathrm{a}} \times$ voltage).

In terms of the electric signals associated to the actuator and the sensor, the control law that implements leaking Integral Force Feedback is given by:

$$U_{\mathrm{act}}(s) = C_{\mathrm{IFF}}^{\mathrm{el}}(s)\, q_{\mathrm{sens}}(s) \tag{9}$$

with:

$$C_{\mathrm{IFF}}^{\mathrm{el}}(s) = \frac{K_{\mathrm{IFF}}^{\mathrm{el}}}{s + p_{\mathrm{IFF}}} \tag{10}$$

in which we have:
- $K_{\mathrm{IFF}}^{\mathrm{el}}$: the gain associated to the high-frequency asymptote of the low-pass filter;
- p_{IFF} : the cut-off frequency of the low-pass filter.

In the middle plot of Fig. 2, the general shape of a leaking IFF-controller is shown, in relation to the location of the resonance frequency of a mechanical structure with a single mode of vibration. The optimal values of the controller parameters depend

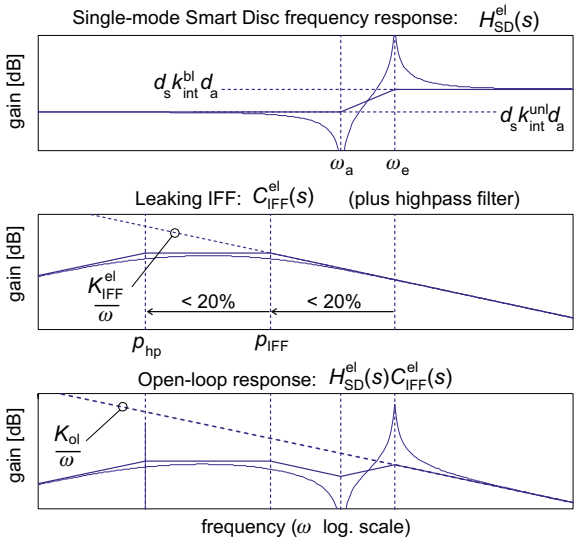

Fig. 2. IFF-controller design, based on the Smart Disc frequency response.

Table 1. Optimal IFF parameters, depending on the relative value of the anti-resonance frequency

	$\omega_a \ll \omega_e$	$\omega_a \approx \omega_e$
K_{IFF}^{el}	$40\% \times \frac{\omega_e}{K_{SD}^{hf}}$	$100\% \times \frac{\omega_e}{K_{SD}^{hf}}$
p_{IFF}	$20\% \times \omega_e$	$5\% \times \omega_e$

on the relative value of the anti-resonance frequency and the resonance frequency of the Smart Disc response. In general they should be chosen in a range according to Table 1 (Holterman, 2002).

Remark. The leaking IFF-controller sketched in Fig. 2 also shows some high-pass behaviour, as indicated by the cut-off frequency p_{hp}. From the perspective of controller design, this behaviour is not necessary. However, in practice high-pass behaviour is inevitable, as it is impossible to perform static force measurements with a piezoelectric sensor. This is due to the fact that over time, the charge built up at the sensor leaks away. As long as the value of the highpass cut-off frequency is chosen sufficiently small ($p_{hp} < 20\% \times p_{IFF}$), the functioning of the controller is hardly affected (Holterman, 2002).

In the lower plot of Fig. 2, the open-loop response of an IFF-controlled Smart Disc system is shown. In order to obtain good damping, the gain of the high-frequency asymptote at the location of the resonance frequency

$$\left.\frac{K_{ol}}{\omega}\right|_{\omega=\omega_e} = \frac{K_{ol}}{\omega_e} = \frac{K_{IFF}^{el} K_{SD}^{hf}}{\omega_e} \qquad (11)$$

should be between –8 and 0 dB (i.e. between 40% and 100% of 0 dB, corresponding to Table 1).

4. CHARGE AMPLIFIER DESIGN FOR INTEGRAL FORCE FEEDBACK

Having illustrated how to tune an IFF-controller for damping a single vibration mode, we will now discuss the incorporation of the controller function within the charge amplifier for the Smart Disc sensor.

Charge amplifier – basic scheme. The basic scheme of a charge amplifier for a piezoelectric sensor is given in Fig. 3a (Tichy and Gautschi, 1980). Assuming infinite amplifier gain A_{amp}, this scheme enforces the voltage across the piezoelectric sensor to zero, by letting the piezoelectric charge flow to the 'feedback' capacitor C_{fb}:

$$i_{fb} = -i_{sens} \qquad (12)$$

The sensor charge thus is effectively converted into a voltage at the output of the amplifier:

$$U_{out} = \frac{1}{C_{fb}} \int i_{fb} \mathrm{d}t = -\frac{1}{C_{fb}} \int i_{sens} \mathrm{d}t = -\frac{1}{C_{fb}} q_{sens} \qquad (13)$$

The transfer function of the charge amplifier in Fig. 3a is characterised by a simple gain (see Fig. 4a):

$$H(s) = \frac{U_{out}}{q_{sens}}(s) = -\frac{1}{C_{fb}} \qquad (14)$$

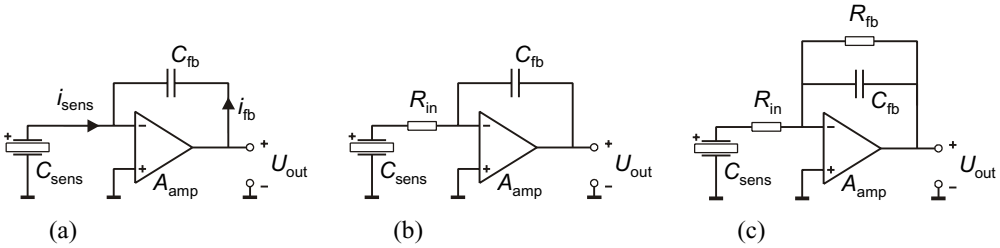

Fig. 3 (a) Basic scheme of a charge amplifier, (b) extended with first-order lowpass behaviour, (c) extended with first-order highpass behaviour. (Remark: the '+' indicates the positive electrode of the sensor.)

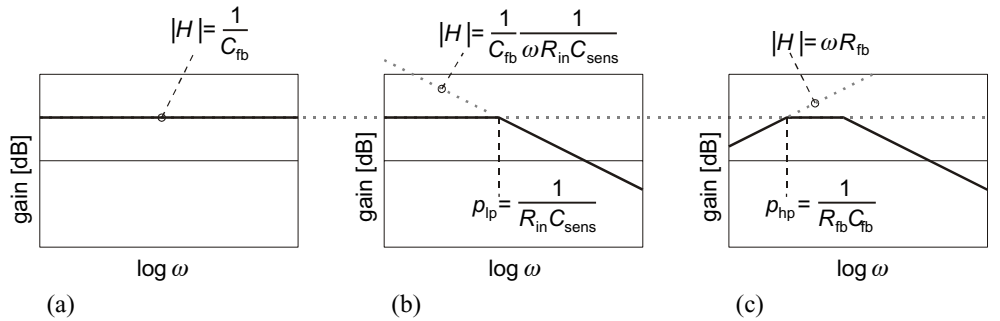

Fig. 4 Frequency response functions (asymptotic approximation) corresponding to the electric circuits in Fig. 3.

Incorporating first-order lowpass behaviour. The charge amplifier as described above can readily be given a well-defined first-order lowpass behaviour, by adding a series resistance R_{in} to the sensor capacitance C_{sens}. The transfer function of the modified amplifier in Fig. 3b reads (see Fig. 4b):

$$H(s) = -\frac{1}{C_{\text{fb}}}\frac{1}{1+sR_{\text{in}}C_{\text{sens}}} \tag{15}$$

with a lowpass cut-off frequency given by:

$$p_{\text{lp}} = \frac{1}{R_{\text{in}}C_{\text{sens}}} \tag{16}$$

Remark. In case of a long cable between sensor and electric circuit, the cable capacitance adds up to the sensor capacitance. This results in a lower cut-off frequency p_{lp} and a lower gain for the high-frequency asymptote.

Incorporating first-order highpass behaviour. In practice the feedback capacitance in a charge amplifier is usually shunted by a (large) resistance R_{fb} (see Fig. 3c), giving the charge amplifier a well-defined first-order high-pass behaviour, characterised by a cut-off frequency given by:

$$p_{\text{hp}} = \frac{1}{R_{\text{fb}}C_{\text{fb}}} \tag{17}$$

The transfer function of the charge amplifier in Fig. 3c reads:

$$H(s) = -\frac{1}{C_{\text{fb}}}\frac{sR_{\text{fb}}C_{\text{fb}}}{1+sR_{\text{fb}}C_{\text{fb}}}\frac{1}{1+sR_{\text{in}}C_{\text{sens}}} \tag{18}$$

The gain plot of this transfer function is illustrated in Fig. 4c. Here it is assumed that the highpass cut-off frequency p_{hp} is chosen smaller than the lowpass cut-off frequency characterised by p_{lp}, i.e., it is assumed that $R_{\text{fb}}C_{\text{fb}} > R_{\text{in}}C_{\text{sens}}$.

Remark. In case $R_{\text{fb}}C_{\text{fb}} < R_{\text{in}}C_{\text{sens}}$ the shape of the response is still given by Fig. 3c. However, the parameters do change, as indicated in Table 2.

5. DESIGN PROCEDURE

The shape of the frequency response function (Fig. 4c) of the charge amplifier in Fig. 3c is identical to the shape of the leaking IFF-controller (with high-pass filter) in the middle plot of Fig. 2. Therefore the charge amplifier can readily be given the function of an IFF-controller, by means of the following design procedure. (Here it is assumed that the sensor has been properly selected and thus C_{sens} is known.)

1. *Determine appropriate values for the IFF-controller parameters $K_{\text{IFF}}^{\text{el}}$ and p_{IFF} as well as an appropriate value for the highpass cut-off frequency p_{hp} (see Fig. 2 and Table 1).*

2. *Calculate the values of the electric components realising the desired controller:*

$$R_{\text{in}} = \frac{1}{p_{\text{IFF}}C_{\text{sens}}} \tag{19}$$

$$C_{\text{fb}} = \frac{p_{\text{IFF}}}{K_{\text{IFF}}^{\text{el}}} \tag{20}$$

$$R_{\text{fb}} = \frac{1}{p_{\text{hp}}C_{\text{fb}}} \tag{21}$$

We will illustrate the above design procedure for an experimental Smart Disc set-up which is used at the University of Twente for demonstration purposes (Holterman *et al.*, 1998). The set-up has been designed such that the dynamic behaviour is dominated by a single vibration mode.

The Smart Disc response of this set-up (i.e., the open-loop transfer from actuator to sensor) is given by the black curve in Fig. 5. The dominant resonance and anti-resonance frequency are found to be 166 Hz and 139 Hz respectively. Additional dynamics can be seen beyond 1 kHz. The alternating pole-zero-pattern is clearly observed.

In determining the Smart Disc response shown in Fig. 5, we have read out the voltage at the sensor rather than the charge. The gain for high frequencies has been found to be –31 dB (0.028 V/V). The value of the high-frequency gain as in (7) can therefore be determined by accounting for the value of the sensor capacitance, which is known to be $C_{\text{sens}} = 7.0$ μF:

$$\begin{aligned} K_{\text{SD}}^{\text{hf}} = \left.\frac{q_{\text{sens}}}{U_{\text{act}}}\right|_{\text{hf}} &= C_{\text{sens}} \cdot \left(-\left.\frac{U_{\text{sens}}}{U_{\text{act}}}\right|_{\text{hf}} \right) \\ &= -7.0 \cdot 10^{-6} \cdot 0.028 \\ &= -0.20 \cdot 10^{-6} \text{ [C/V]} \end{aligned}$$

Table 2 Characteristic parameters of the modified charge amplifier shown in Fig. 3c

	gain of $H(s)$ for $\omega < p_{\text{hp}}$	p_{hp}	gain of $H(s)$ for $p_{\text{hp}} < \omega < p_{\text{lp}}$	p_{lp}	gain of $H(s)$ for $\omega > p_{\text{lp}}$
$R_{\text{fb}}C_{\text{fb}} > R_{\text{in}}C_{\text{sens}}$ (see Fig. 2.c)	ωR_{fb}	$\frac{1}{R_{\text{fb}}C_{\text{fb}}}$	$\frac{1}{C_{\text{fb}}}$	$\frac{1}{R_{\text{in}}C_{\text{sens}}}$	$\frac{1}{C_{\text{fb}}} \cdot \frac{1}{\omega R_{\text{in}}C_{\text{sens}}}$
$R_{\text{fb}}C_{\text{fb}} < R_{\text{in}}C_{\text{sens}}$		$\frac{1}{R_{\text{in}}C_{\text{sens}}}$	$\frac{R_{\text{fb}}}{R_{\text{in}}C_{\text{sens}}}$	$\frac{1}{R_{\text{fb}}C_{\text{fb}}}$	

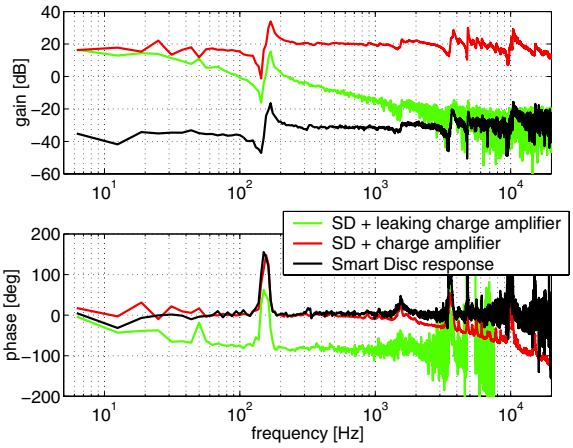

Fig. 5. Illustration of the design procedure for the experimental Smart Disc set-up.

In accordance to the guidelines in Table 1, we have aimed for an IFF-controller characterised by:

$$p_{\mathrm{IFF}} = 10\% \times \omega_{\mathrm{e}} = 0.1 \cdot 2\pi \cdot 166 = 104\,[\mathrm{rad/s}] \;\; (=17\ \mathrm{Hz})$$

$$K_{\mathrm{IFF}}^{\mathrm{el}} = 100\% \times \frac{\omega_{\mathrm{e}}}{\left|K_{\mathrm{SD}}^{\mathrm{hf}}\right|} = \frac{2\pi \cdot 166}{0.20 \cdot 10^{-6}} = 5.2 \cdot 10^{9}$$

$$p_{\mathrm{hp}} = 10\% \times p_{\mathrm{IFF}} = 0.1 \cdot 104 = 10.4\,[\mathrm{rad/s}] \;\; (=2\ \mathrm{Hz})$$

Remark. In calculating the IFF-gain, we have left out the minus sign. By properly connecting the amplifier and the actuator a minus sign can be introduced again.

With (19–21) we have found the following values:

$$R_{\mathrm{in}} = 1/(p_{\mathrm{IFF}} C_{\mathrm{sens}}) = 1/(104 \cdot 7.0 \cdot 10^{-6}) = 1.37\,[\mathrm{k\Omega}]$$

$$C_{\mathrm{fb}} = p_{\mathrm{IFF}} / K_{\mathrm{IFF}}^{\mathrm{el}} = 104 / 5.2 \cdot 10^{9} = 20\,[\mathrm{nF}]$$

$$R_{\mathrm{fb}} = 1/(p_{\mathrm{hp}} C_{\mathrm{fb}}) = 1/(10.4 \cdot 20 \cdot 10^{-9}) = 4.8\,[\mathrm{M\Omega}]$$

First we have realised the basic charge amplifier function (Fig. 3a). The frequency response is given by the upper (red/dark grey) curve in Fig. 5. The observed gain (about 50 dB, compared with the original response) is given by the ratio of the sensor capacitance and the feedback capacitance:

$$\frac{U_{\mathrm{out}}}{U_{\mathrm{act}}} = -\frac{1}{C_{\mathrm{fb}}} \frac{q_{\mathrm{sens}}}{U_{\mathrm{act}}} = \frac{C_{\mathrm{sens}}}{C_{\mathrm{fb}}} \frac{U_{\mathrm{sens}}}{U_{\mathrm{act}}} \qquad (22)$$

with $C_{\mathrm{sens}} / C_{\mathrm{fb}} = 7.0 \cdot 10^{-6} / 20 \cdot 10^{-9} = 350$ $(= 51\ \mathrm{dB})$.

Remark 1. The operational amplifier that is used in this experiment can not realise such a high gain for high frequencies, which can be deduced from the phase that drops beyond 2 kHz.
Remark 2. In order to facilitate the measurement, the feedback resistor R_{fb} has been incorporated already in the amplifier circuit. Its influence on the measured frequency response however can not be seen, as the cut-off frequency is too low (2 Hz).

The first-order lowpass behaviour is realised by adding the input resistance (Fig. 3b), which yields the desired –20 dB/dec slope beyond 17 Hz (green/light grey curve in Fig. 5). In the frequency region of interest, the phase can be seen to vary between –90° and +90°. The high-frequency asymptote can be seen to cross the 0 dB-level in the vicinity of the resonance frequency ω_{e}, as required (see section 3, Table 1).

Upon application of the amplifier output voltage to the Smart Disc actuator, the analog controller has shown excellent damping behaviour: the damping ratio increased from 0.5% to about 10%.

5. CONCLUSION

In this paper it has been shown that a piezoelectric actuator and a collocated piezoelectric sensor can readily be used as an active damping element. The electric circuit for realising active damping has been reduced to a single operational amplifier with three electric components. The values of these components can be determined via a straightforward design procedure. Experiments on a laboratory set-up have confirmed the adequacy of this procedure, as well as the robustness of the control approach that has been used for active damping.

REFERENCES

Holterman, J. (2002). *Vibration Control of High-precision Machines with Active Structural Elements*, PhD thesis, University of Twente, Twente University Press, Enschede, The Netherlands. http://www.ce.utwente.nl/smartdisc

Holterman, J., T.J.A. de Vries, and M.P. Koster (1998), 'Experiment to evaluate the feasibility of the Smart Disc concept', Proc. 6th UK Mechatronics Forum International Conference 'Mechatronics'98', Skovde, Sweden, pp. 217-222.

Preumont, A., J.P. Dufour, and C. Malékian (1992). 'Active Damping by a Local Force Feedback with Piezoelectric Actuators', *AIAA Journal of Guidance, Control and Dynamics*, **15**(2), pp. 390-395.

Preumont, A. (1997). *Vibration Control of Active Structures*, Kluwer Academic Publishers, Dordrecht, The Netherlands.

Tichy, J. and G.H. Gautschi (1980). *Piezoelektrische Meßtechnik: Physikalische Grundlagen, Kraft-, Druck- und Beschleunigungsaufnehmer, Verstärker*, Springer-Verlag, Berlin, Germany.